The measurement of arrow velocities in the students' laboratory[1]

C. Tuijn and B.W. Kooi

Abstract

A method is described for measuring arrow velocities by means of the induction voltages, evoked by shooting arrows with a magnetized point through two coils at a fixed distance. Small effects such as the influence of string material, number of strands, bracing height and stabilizers can be detected. The experimental set-up is relatively simple and can be used in an early stage of the student's laboratory course. Some results for modern competition bows are presented. Possibilities for model calculations are discussed.

[1] *European Journal of Physics* **13**: 127–134 (1992)

1 Introduction

The invention of the bow and arrow may rank in social impact with the invention of the art of kindling and the invention of the wheel. It must have been in prehistoric times that the first missile was launched with a bow. We do not know where and when. This may be the reason that for many students the system of bow and arrow is interesting (besides their interest for projectiles in general).

The laboratory course for undergraduate students in physics in their first year at the University of Amsterdam ends with a 'free' experiment. 'Free' means that the students work at an experiment of their own choice, and that the experiment is open-ended. Recently one of our students, who is a competition archer, proposed to measure the velocity of arrows under different circumstances. The method he proposed uses the voltage that is induced by the magnetized point of an arrow, when the arrow flies through two coils at a fixed distance. This method appeared to be very accurate and gave a number of interesting results.

For calculations on the system of bow and arrow, models have to be made. In the 1930s Hickman, Klopsteg and Nagler not only performed experiments on different designs of the bow, but they also developed models. As part of modelling simplifying assumptions had to be made in order to obtain a solution in closed form or to approximate the solution of the governing equations numerically in an acceptable amount of computing time. Because of these simplifications only bows with specific features could be described. In Section 4 we discuss some of these models in more detail.

2 Experimental set-up

The velocity of the arrows was determined by measuring the time of flight between two coils 2 metres apart. The first coil was placed at some distance from the bow, varying from 0.5 to 3 m. The coils used had nearly 400 windings of 0.2 mm copper wire on wooden formers with an aperture of 16.5 cm diameter. For an experienced archer it is no problem to shoot the arrows through both of the coils. To improve the experimental conditions we installed a heavy rack to which the bow and the release were attached. This release is a mechanical device which clamps the string with a small loop of cord, and which looses the arrow in a very reproducible way when a button is depressed.

In each experimental situation a series of 12 shots was made, from which the average and the standard deviation were calculated. The accuracy mentioned between brackets is always the standard deviation of the set of measurements.

When shooting from hand the arrow is placed under a small clamp on the grip, the clicker. When the arrow is drawn it is glides under this clamp until the becomes free from it, and a little click is heard: the arrow is at the clicker point. This is the moment the arrow has reached its final draw length and has to be released. For shooting from the rack the mechanical release was mounted at a fixed distance relative to the grip, so we did not have to use this clicker.

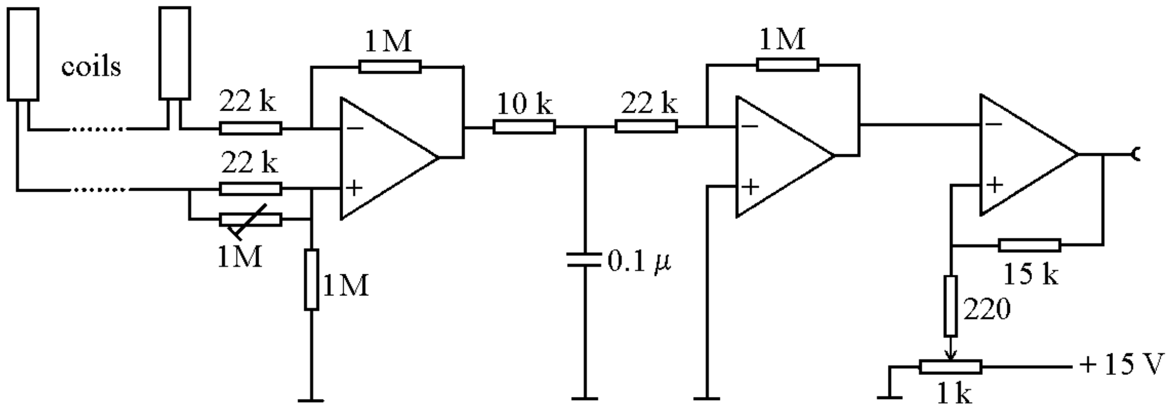

Figure 1: Electronic circuit with 3 opamps of type 741, forming two amplifiers and a Schmitt trigger. The variable resistor of 1 MΩ serves to make the ratio of the resistors of the first opamp exactly equal to obtain a high common mode rejection ratio.

The induction voltages were amplified by a differential amplifier, built with two opamps of type 741, as indicated in Figure 1. An opamp Schmitt trigger, adjusted at a small positive level and zero level, gave the edges necessary for starting and stopping the timer. To check the signal a transient recorder was connected to the output of the amplifier. An example of these signals is shown in Figure 2.

The time dependence of the voltage induced in the coil depends on the place where the arrow flies through the coil. At the moment that the induction voltage goes through zero with a very sharp edge, the point of the arrow must be very close to the median plane of the coil. Since the same applies to both coils, the distance is defined very precisely. The point of the arrow was magnetized by attaching it for some time to the pole of a permanent magnet. For shooting from hand the bows were equipped with stabilizers. All measurements were performed indoors.

The force-draw curves were determined by hanging the bow on a hook and loading it with different masses on a scale. The masses had been measured very precisely (better than 0.1%). The distance of draw was measured with a steel measuring staff with a millimetre division, whose accuracy is better than 0.25%.

Other methods for measuring the velocity are photography with a high speed camera, determining flight distance and the ballistic pendulum. Nowadays, video recording is also possibility, but none of the methods can attain the accuracy of our method. Maybe the method used for measuring muzzle velocities of bullets, where the bullet passes through two 'planes' of laser bundles may equal our precision.

Figure 2: The form of the induction voltage and the Schmitt trigger levels.

3 Results and discussion

The bows we used are specified in Table 1. The specifications have the following meaning. For example the OK Bow 68” 38.5# has a top to bottom length of 1.73 m (68”) and needs, according to the manufacturers specifications, a force (called weight by archers) of 171 N (38.5 lbs) for complete draw. We call this the nominal weight. The code CV means that the limbs have been reinforced with carbon fibres. The arrows we used were all aluminum Easton arrows, with the appropriate length for each bow.

For bows OK1 and GH we determined the force-draw curves with increasing and decreasing load; for the other bows with increasing load only. The hysteresis was less then 1%, see Table 1. Maybe these results are not completely reliable, because of the process of putting masses on the scale and taking them off again to exchange them with heavier ones. The relaxation of the material of the limbs may have been enhanced by this process. The calculation of the energy, being the area below the force-draw curve, was done with the trapezoid formula for numerical integration. The form of the curves is not very different from that of the curves published formerly [1–4].

Since the method for the measurement of the velocity appeared to be very accurate (most series of shots gave a standard deviation of about 0.2% or less in the measured velocities), it was possible to detect small effects. On the other hand it was difficult to control all design parameters of the bow-arrow combination, such as the bracing height (the distance between the undrawn string and the grip of the bow, $|OH|$ in Figure 3), the length of draw and the way of releasing. The difference in shooting from hand and from the rack was surprisingly large: the velocity of arrows shot from the rack was 3% higher.

Table 1: Bows used. *) has not been measured.

Acronym	OK1	OK2	OK3	GH
Make	OK	OK	OK	Greenhorn
Name	Match	Match	Match	Comet
Specification	superflex CV	superflex CV	superflex CV	TD 350
Type	68" 38.5#	70" 34#	66" 40#	68" 30#
Eff. draw [cm]	43.0	50.9	44.0	42.9
Nom. weight [N]	171	151	178	133
Eff. Weight [N]	170.5	170	178	130
Bracing ht [cm]	21.8-22	21.9	*)	21.4-22
W [J]	42.6	50.3	45.6	33.2
Hysteresis [%]	0.2	*)	*)	0.9

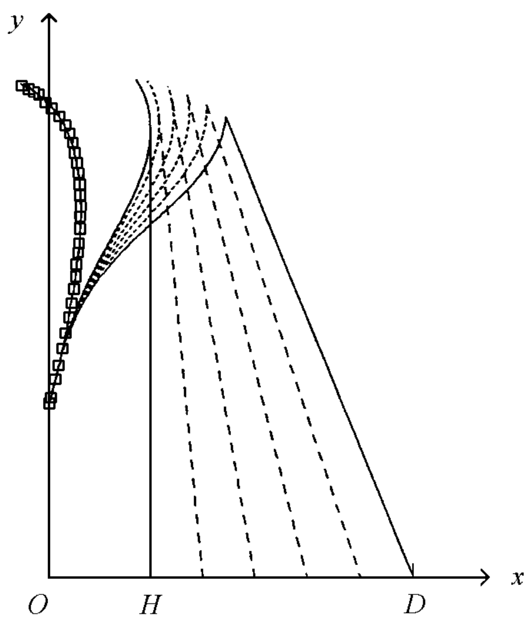

Figure 3: Different situations of the working-recurve bow; the upper half of the bow is shown. The x-axis coincides with the line of aim. O: unbraced (squares are stations for measurement of the shape); H: braced and D: fully drawn.

Table 2: Velocity as a function of the number of strands. Fast Flight string on GH.

Number of strands	Mass (g)	Velocity (m/s)
16	6.45	51.88 (6)
14	5.82	51.43 (6)
12	5.28	51.62 (10)
10	4.64	51.76 (7)

Possibly during loosing by hand the length of draw is not precisely defined: the string is sliding along the finger-tips, so the energy transferred to the arrow will be less than when released in a mechanical way. Another cause may be that the bow hand is yielding a little during the shot. Further the arrows loose energy during their flight because of the friction with the air. For different arrows the loss of velocity in the first 5 m appeared to vary from 0.25% per metre to 0.5% per metre. Since the distance to the first coil was 0.5 to 1 m for shooting from the rack and about 3 m for shooting from hand, this explains a part of the difference. This also means that the real initial velocity, defined as the velocity of the arrow at the moment it leaves the string, was a little higher: about 1 to 2% for shooting from hand, and 0.5 to 1% for shooting from the rack. These small corrections have not been applied to the data in the tables and figures. small

One of the small effects we could detect is the influence of the stabilizers. Modern competition bows are equipped with several stabilizing elements to reduce rotations and other movements of the bow. This is shown in Figure 4. With complete stabilization the velocity is highest. Since the inertial mass of the stabilizers reduces the movement of the bow hand this is in agreement with the above mentioned yielding of the bow hand. Perhaps more important for target shooters is the result that the standard deviation is smallest with complete stabilization.

The effect of different string masses on the velocity has already been investigated by Hickman et al. [2, pp.45-47]. His conclusion was that the effect depends on the specifications of the bow, and that 'the velocity of an arrow is reduced about the same amount as if the arrow were increased in weight by one-third the increase in weight of the string.' This can easily be explained if it is assumed that at arrow exit the ends of the string are in rest, the centre of the string has the same velocity as the arrow and the parts between have a velocity that linearly depends on the position along the string.

Yet the string can be subject of several investigations. In [6] it was pointed out that there are two counteracting effects: on one hand the velocity is higher when the string is lighter; on the other hand the thicker the string, the stiffer it is, and the higher the velocity. We prepared a Fast Flight string of 16 strands and removed consecutively two, four and six of its strands. In Table 2 it is shown that the differences are small. To exclude the effect of the mass of the string, we prepared strings of different materials, but with almost the same mass. In Table 3 the results indicate that the Dacron strings give a distinctly lower

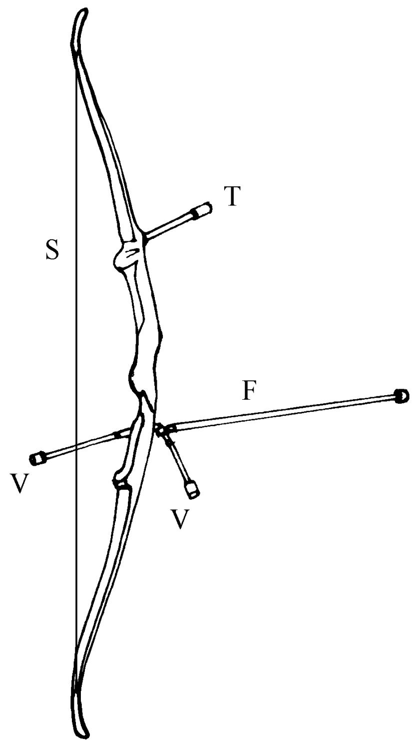

Figure 4: Stabilizing elements of the bow: S is string, T is top stabilizer, F is front stabilizer and V is V-bar. T and F are in the vertical plane of the bow, F pointing horizontally forward and T slantwise forward. V is in an almost horizontal plane, with both legs pointing a little backwards and a little downwards.

velocity. This is in agreement with its lower modulus of elasticity [6, p.119]. For Dacron B50 and Kevlar the force to elongate a string was determined: for Dacron the force is about 22 N per % of elongation per strand; for Kevlar 70 N per % per strand. Twaron too is known for its high stiffness. Apparently the Fast Flight strings are best; the material is Dyneema SK60.

An important quantity for the archer is the bracing height. This distance determines the amount of energy to be stored in the bow during drawing the arrow until the full draw. Therefore archers always measure this bracing height very precisely to secure reproducibility of the shots. Since it depends rather strongly on the length of the string, and strings may tend to yield a little when they are strung, sometimes the archer has to correct the length of the string by twisting it. By doing so the elastic properties are changed a bit, but probably this is a minor effect. To investigate the effect of bracing height, we followed the same procedure. We used one string and twisted it a number of times. Strangely enough the force at full draw does not change very much, though the string is shorter. This fact was discovered by Hickman [2, pp.18-21]. We illustrate it in Figure 5(a) with the force-draw curve of the Greenhorn bow for different bracing heights. This means that the amount of elastic energy W stored in the limbs is roughly a linear function of the bracing height b: the larger b, the smaller W, because the effective draw length decreases. If now the efficiency (the ratio of the kinetic energy of the arrow at exit and the elastic energy stored in the bow before release of the arrow) does not depend on the bracing height, the kinetic energy of the arrow will also be a linear function of the bracing height. In Figure 5(b) we have plotted the kinetic energy of the arrow, (T_a), as a function of the bracing height for the OK1 bow. The slope of the line is $-95(4)$ J/m, which means that the dependency of the apparent efficiency on variations in bracing height is about 2% per cm for this bow.

Klopsteg [3] improved Hickman's rule by stating that a certain part r of W, the de-

Table 3: The velocity, kinetic energy T_a and the efficiency for different strings: a) from hand with OK3 and complete stabilization, arrow mass 20.1 g; b) from rack with GH, no stabilizers, arrow mass 18.1 g.

String	Mass [g]	Velocity [m/s]	T_a [J]	Eff. [%]
a)				
Dacron	6.10	55.44 (12)	30.8	68.0
Kevlar	5.95	58.07 (5)	33.8	74.0
Twaron	5.55	57.77 (10)	33.5	73.0
FastFlight	6.02	58.38 (12)	34.2	75.0
b)				
Dacron	6.55	49.73 (4)	22.5	70.0
Kevlar	6.48	51.25 (10)	23.9	73.8
Twaron	6.53	51.68 (7)	24.3	75.0
FastFlight	6.45	52.09 (9)	24.7	76.2

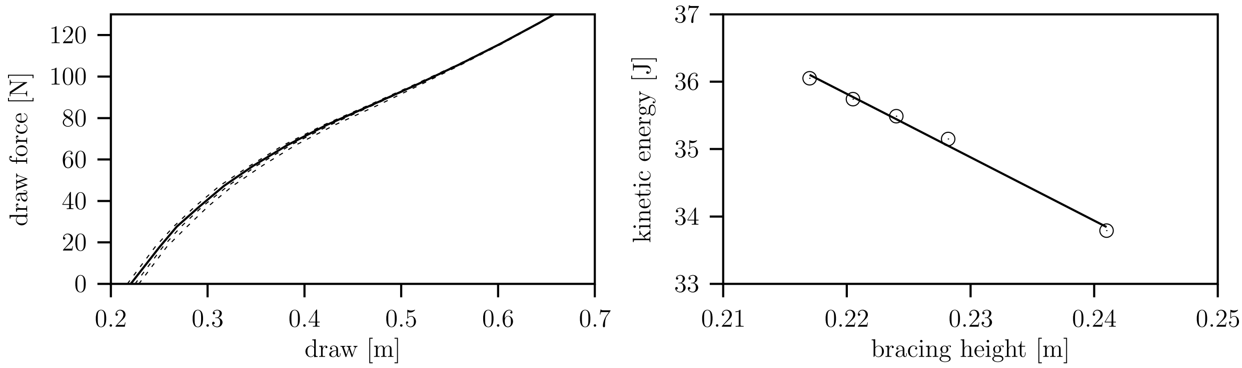

a) b)

Figure 5: a) The force-draw curve for four different bracing heights of the GH bow with Dacron string. b) The kinetic energy T_a as a function of the bracing height for the OK1 bow.

Table 4: Arrow mass dependence of velocity. Arrows shot from the rack. Linear least squares fit for $2\,W/v^2 = (m+K)/r$. Note: The OK bow was used with higher effective weight than nominal; the Greenhorn bow slightly lower.

Bow	OK2	GH
String	FF	Dacron
W [J]	50.3	33.2
K [g]	5.8 (5)	9.2 (5)
r	1.02 (2)	1.04 (2)

formation energy of the bow (and string), is converted to kinetic energy of the arrow, the string and the bow limbs:

$$rW = \frac{1}{2}(m+K)v^2 \tag{1}$$

where r is a number < 1, because there is some energy loss by hysteresis, m is the arrow mass and K represents one third of the string mass plus an unknown added mass, accounting for the kinetic energy of the limbs. In fact K also accounts for the excess of elastic energy in the limbs and the string at arrow exit compared with the undrawn, braced situation. In principle some added mass of air, that is dragged with the arrow, string and limbs will be included in K also. K is called virtual mass. Experimentally Klopsteg showed that K is a constant for a specific bow. In fact K is a phenomenological quantity that cannot simply be identified with physical properties of the bow. K can be determined by measuring the velocity as a function of arrow mass.

We measured the arrow mass dependence of the velocity for two bows. Some arrows were prepared with higher masses by moulding polymer material into the points. The results are summarized in Table 4. To find r and K we applied a linear least squares fit of $2\,W/v^2$ as a function of m, see Figure 6. The values of r are striking, they mean that a very small amount of energy is lost in hysteresis. This agrees well with the low values for the hysteresis we found with the force-draw curves.

4 Mathematical models

The first model developed is Hickman's model [2, pp.13-17] of a straight-end bow, which consists of a straight rod of wood, bent by placing the string. The position of the bow is specified in an Cartesian coordinate system (x, y), the line of symmetry of the bow coinciding with the x-axis and the origin O coinciding with the midpoint of the bow, analogous to the situation for the working-recurve bow in Figure 3. The limbs of the bow are assumed to have a uniform thickness and their width tapers to the tips. In that case the bending stiffness is given by $EI(s) = EI(0)\,(L-s)/L$ where E is Young's modulus, I

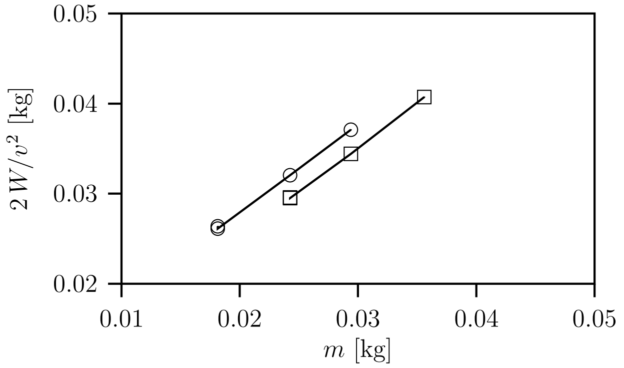

Figure 6: Klopsteg's rule: the mass dependence of the kinetic energy for the OK2 bow (□) and the GH bow (○). Linear least squares fit for $2\,W/v^2 = (m + K)/r$.

is the second moment of inertia and s is the length parameter along the limb with $s = 0$ in the origin and $s = L$ at the tip. The mass per unit of length is $\rho C(s) = \rho C(0)(L - s)/L$, where ρ is the density and $C(s)$ is the area of the cross-section. The mass of one limb is then given by

$$m_b = \int_0^L \rho C(s)\, ds = \frac{1}{2}\rho C(0)L\ . \tag{2}$$

The relationship between the loading and the deformation is derived by use of the Euler-Bernoulli equation:

$$\frac{d^2x}{ds^2} = \frac{M}{EI} \tag{3}$$

where M is the bending moment at s. When the limb is deformed by a force F perpendicular to the limb at the tip, while it is clamped in the center of the bow, integration gives for small deformations, after substitution of $I(s)$ and $M = F\,(L - s)$:

$$x(s) = \frac{F L}{2\,EI(0)}\, s^2 \tag{4}$$

or

$$x(s) = \frac{x(L)s^2}{L^2} \tag{5}$$

In order to get a simplified model for the dynamics we assume that the shape of the moving limb equals at each moment the shape of the limb deformed by the force F giving the same deflection of the tip given by equation (4). In that case there is a simple relationship independent of time between the position of the tip $x(L,t)$ and of all the other points along the limb, see equation (5). The kinetic energy is

$$A_T = \frac{1}{2}\int_0^L \rho C(s)\left(\dot{x}(s,t)\right)^2\, ds = \frac{1}{2}\frac{1}{15}m_b\left(\dot{x}(L,t)\right)^2 \tag{6}$$

and the potential energy equals

$$A_P = \frac{1}{2}\int_0^L \frac{M^2}{EI}\,ds = \frac{EI(0)}{L^3}x(L,t)^2\ . \tag{7}$$

Hence we end up with a one degree of freedom system of which the state variable is the deflection $x(L,t)$ of the tip. This is because of the relationship between $x(s,t)$ and $x(L,t)$ which is independent of the time t. The equation of motion can be derived using the Lagrangian formalism, with the Lagrangian function $\mathcal{L}(\dot{x}(L,t), x(L,t))$ for the conservative system:

$$\mathcal{L} = A_T - A_P = \frac{1}{2}\frac{1}{15}m_b\left(\dot{x}(L,t)\right)^2 - \frac{1}{2}\frac{EI(0)}{L^3}x(L,t)^2\ . \tag{8}$$

$$\frac{d}{dt}\frac{\partial\mathcal{L}}{\partial\dot{x}(L,t)} - \frac{\partial\mathcal{L}}{\partial x(L,t)} = 0\ . \tag{9}$$

$$\frac{1}{15}m_b\left(\ddot{x}(L,t)\right) + \frac{2\,EI(0)}{L^3}x(L,t) = 0\ . \tag{10}$$

This result shows that the equations of motion can be interpreted in terms of a lumped model. The mass of the limb is represented by a mass $m_b/15$ at the tip of the limb and the flexible limb is replaced by a massless rigid rod of length L, connected with an elastic hinge to the grip at $s = 0$. The elastic hinge is a composition of a smooth hinge with a clock spring with elastic constant $k = 2\,EI(0)/L$.

Now Hickman did not place the hinge at the clamped end ($s = 0$), but at $s = 1/4\,L$ because he noticed that the trajectory of the tip is an arc of a circle with its centre at $s = 1/4\,L$ on the unbent limb. Then the elastic constant becomes $k = 18/16\,EI(0)/L$. To derive the place of this point he used the fact that for small deflections the form of the bent limbs is nearly an arc of a circle. Let the radius of this circle be r, then we have the following parametric representation for the curve of the tip:

$$x(L) = r\big(1 - \cos(\frac{L}{r})\big) \quad \text{and} \quad y(L) = r\sin(\frac{L}{r})\ . \tag{11}$$

The radius R of this curve is given by

$$R = \left|\frac{\left(\left(x'(L)\right)^2 + \left(y'(L)\right)^2\right)^{3/2}}{x'(L)y''(L) - y'(L)x''(L)}\right| \tag{12}$$

where for instance x' denotes dx/dr. For $\lim r \to \infty$ we have $R = 3/4\,L$, and this shows that the trajectory of the tip and the trajectory of the tip in the hinge model are in good agreement when the position of the hinge is placed at $s = 1/4\,L$.

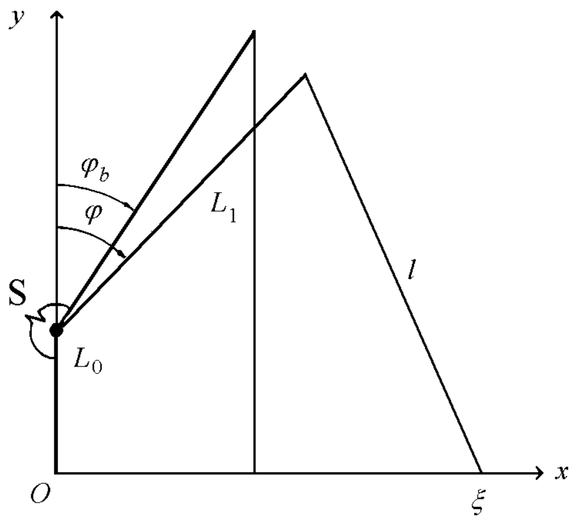

Figure 7: Geometry of the bow in Hickman's model.

We are now in the position to derive the governing equations for the lumped parameter model. From Figure 7 we find for the x coordinate, ξ, of the midpoint of the string, where the arrow with mass $m = 2\,m_a$ is placed:

$$\xi = L_1 \sin\varphi + \left(l^2 - (L_0 + L_1\cos\varphi)^2\right)^{1/2} . \tag{13}$$

The half length of the string is l, L_0 is the half length of the grip, equal to $1/4\,L$ in Hickman's model, and L_1 is the length of the rod, equal to $3/4\,L$. Finally π is the angle of rotation of the rod. When the unstrung bow is straight, we take the unloaded hinge for $\varphi = \varphi_0 = 0$. The Lagrangian for the upper half of the bow is, using the coordinates φ and ξ:

$$\mathcal{L} = \frac{1}{2} J\dot{\varphi} + \frac{1}{2}\,m_a\dot{\xi}^2 - \frac{1}{2}\,k\varphi^2 . \tag{14}$$

where J is the moment of inertia of the limb with respect to pivot point S. Due to equation (13) we have one superfluous coordinate, which should be eliminated. Equation (13) gives

$$\dot{\xi} = Q\dot{\varphi} , \tag{15}$$

with

$$Q = L_1\cos\varphi + L_1\sin\varphi\frac{(L_0 + L_1\cos\varphi)}{\left(l^2 - (L_0 + L_1\cos\varphi)^2\right)^{1/2}} , \tag{16}$$

Substitution of this result in Lagrange's equation yields the equation of motion:

$$(J + m_a Q^2)\ddot{\varphi} + m_a Q\frac{dQ}{d\varphi}\dot{\varphi}^2 + k\,\varphi = 0 . \tag{17}$$

The initial conditions are fixed by the solution of the static problem, where ξ equals the draw length $|OD|$.

$$\xi_f = |OD| = L_1\sin\varphi_f + \left(l^2 - (L_0 + L_1\cos\varphi_f)^2\right)^{1/2} , \tag{18}$$

where the subscript f indicates the fully drawn situation. The equation of equilibrium becomes:

$$\frac{1}{2}F(|OD|)Q(\varphi_f) = k\varphi_f \ , \tag{19}$$

where $F(|OD|)$ is the weight of the bow. The initial velocity of rotation is zero: $\dot{\varphi} = 0$

In this model the arrow leaves the string for $\phi = \phi_b$, where the subscript b indicates the braced situation, when

$$l = (L_0 + L_1 \cos\varphi_b) \tag{20}$$

In [6] it was shown that in this model the bow converts all of the deformation energy of the elastic hinge into kinetic energy of the arrow. The energy integral of the system gives the solution of the equation of motion:

$$\frac{1}{2}(J + m_a Q^2)\dot{\varphi} + \frac{1}{2}k\varphi^2 = \frac{1}{2}k\varphi_f^2 \tag{21}$$

(Note that for $\varphi = \varphi_b$, $Q = \infty$, but that $Q\dot{\varphi} = \dot{\xi}$ is finite.) This completes the derivation of Hickman's model with a massless string. The mass of the string can easily be incorporated in the model by placing one third of its mass at the midpoint of the string and the rest at the ends. The extension of this model with an elastic string, obeying Hooke's law, introduces an extra state variable, so the model becomes two degrees of freedom, for instance the half-length of the string and the position of the arrow. The obtained equations look similar to those derived by Marlow [10] and are not reported here. They should be solved numerically, with a Runge-Kutta method for example.

Marlow [10] described a lumped mass model for the longbow. Unfortunately he let the limb rotate as a rigid body about the beginning of the limb at the place where it meets the grip. In that case for the bow described above the tip mass representing the mass of the limb, becomes $m_b/6$ instead of $m_b/15$, which makes the dynamic behaviour less realistic [6, p.111]. On the other hand Marlow introduced an elastic string to get a more realistic model as to the efficiency. He treated the string as a rod rigid with respect to shear and bending but elastic in the length direction as given by Hooke's law. This explains why in his model the arrow leaves the string while the string is already through its stretched position. This can be considered as an artefact of the model. A string is not capable to withstand shear forces, so it seems better to use a simple lumped mass model for the string. A more general model is obtained when the motion of the limb is described as a vibrating beam undergoing large displacements. The mathematical model is formed by a set of coupled partial differential equations with initial and boundary conditions. With modern working-recurve bows the phenomenon that the string lies during a part of the draw along the limb, see Figure 3, makes the mathematical treatment much more complicated. The place where the string contacts the limb has to be determined as part of the solution. Problems of this type are called free and moving boundary problems for the static and dynamic case respectively. The description of such a model is beyond the scope of this

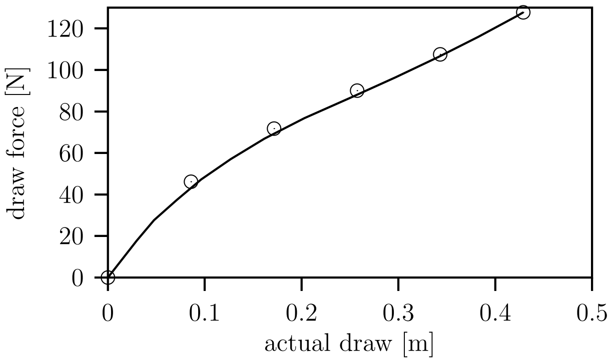

Figure 8: Comparison of the predicted and measured static force-draw curve of the GH bow, after matching of predicted and measured weights (○= predicted values).

Table 5: Comparison of experiment and model calculation for the GH bow. Effective weights have been matched. Hysteresis has not been taken into account. Arrow mass 18.1 g; string mass 6.55 g and string stiffness 260 N per % of elongation (Dacron B50).

	Measured	Predicted
Eff. weight [N]	126.9	126.9
W [J]	32.16	32.9
Kin. energy [J]	22.57	23.9
Eff. [%]	70.2	72.9

paper. The reader is referred to [5–9]. To show the merits of such a model, the calculated and measured force-draw curves of the Greenhorn bow are compared in Figure 8. Since the predicted weight of the bow was too high, a knockdown factor was used for the bending stiffness of the limbs, such that the calculated weight became equal to the measured one. Such an adaptation is usual in this kind of modelling, since the size of different parts of the bow, especially the thickness of the thin layers of fibre-glass cannot be measured precisely. The comparison of measured and predicted values is summarized in Table 5. The predicted efficiency is about 2% too high. In the model no internal or external damping is taken into account. This may explain part of the discrepancy. These results indicate that the model is good enough to use it for, for example, sensitivity analysis as part of the design process of bows.

Schuster [11] made a model for the working-recurve bow too. He made two unrealistic assumptions, namely that the working-recurve is in the form of a circular arc which unrolls along an initial tangent and that this is the only part of the bow that 'works'. The advantage of Schuster's model is that the mathematical treatment is simpler.

5 Conclusion

For teaching purposes our measuring method is very suitable. If it is possible to install some kind of rack to attach the bow, aiming is no longer necessary, for the coils can be placed precisely in the trajectory of the arrows. Our rack was found in a storeroom for cast-off equipment. Some minor adaptations were sufficient to make it a shooting device. The electronic circuit is rather simple. The transient recorder might be a problem to get, but it is advisable to use one during the start of the measurements to be sure to have signals of the right sign. Care is needed to ensure that the arrow point is always magnetized on the same pole of the permanent magnet.

Marlow [10] already pointed out that experiments on archery can be done on different levels and in a great variety. In the appendix of his paper he indicated several possibilities. If one should want to skip the experimental phase, video productions are now available from companies of teaching materials [12], but accurate measurements as described in this paper are not (yet) possible with this kind of production. With our method small effects can be detected, such as the differences arising from string material and stabilizer configuration.

Marlow also mentioned several possibilities for applications of mechanics. For model calculations we discuss different models of different degree of complexity. The Lagrangian method reduces the entire field of statics and dynamics to a simple procedure. In this way the dynamics of the bow and arrow is a beautiful illustration of several notions of mechanics.

Acknowledgements

Firstly we want to express our gratitude to our student, Laurens de Lange, who invested, after finishing his free experiment, much more time in these measurements. Further we thank his colleague archer Pim Pouw, who was very interested in this experiment, and spent a lot of time in the realization of the set-up and the measurements. Also we thank dr. C. Prins, who kindly put at our disposal some masses and a precision balance.

References

[1] C. N. Hickman. The dynamics of a bow and arrow. *J. of Applied Physics*, 8:404–409, 1937.

[2] C. N. Hickman, F. Nagler, and P. E. Klopsteg. *Archery: the technical side.* National Field Archery Association, Redlands (Ca), 1947.

[3] P. E. Klopsteg. Physics of bows and arrows. *Am. J. Phys.*, 11:175–192, 1943.

[4] P. E. Klopsteg. Bows and arrows: a chapter in the evolution of archery in America. Technical report, Smithsonian Institute, Washington, 1963.

[5] B. W. Kooi. On the mechanics of the bow and arrow. *Journal of Engineering Mathematics*, 15:119–145, 1981.

[6] B. W. Kooi. *On the Mechanics of the Bow and Arrow.* PhD thesis, Rijksuniversiteit Groningen, 1983.

[7] B. W. Kooi. The 'cut and try' method in the design of the bow. In H. A. Eschenauer, C. Mattheck, and N. Olhoff, editors, *Engineering Optimization in Design Processes*, volume 63 of *Lecture Notes in Engineering*, pages 283–292, Berlin, 1991. Springer-Verlag.

[8] B. W. Kooi. On the mechanics of the modern working-recurve bow. *Computational Mechanics*, 8:291–304, 1991.

[9] B. W. Kooi and J. A. Sparenberg. On the static deformation of a bow. *Journal of Engineering Mathematics*, 14:27–45, 1980.

[10] W. C. Marlow. Bow and arrow dynamics. *Am. J. Phys.*, 49:320–333, 1981.

[11] B. G. Schuster. Ballistics of the modern-working recurve bow and arrow. *Am. J. Phys.*, 37:364–373, 1969.

[12] Kansas State University. Physics of sports. Available from Videodiscovery, P.O. Box 85878, Seattle, WA 98145-1878. Video.